

All-optical AND gate by use of a Kerr nonlinear microresonator structure

Suresh Pereira, Philip Chak, and J. E. Sipe

Department of Physics, University of Toronto, 60 St. George Street, Toronto M5S 1A7, Ontario, Canada

Received November 5, 2002

We numerically demonstrate the feasibility of constructing an all-optical AND gate by using a microresonator structure with Kerr nonlinearity. The gate is much smaller than similar AND gates based on Bragg gratings and has lower power requirements. © 2003 Optical Society of America

OCIS code: 060.1810.

We consider all-optical switching in the device shown in Fig. 1(a), which consists of two channel waveguides coupled by Kerr nonlinear microresonators.¹⁻⁴ Using the two channels as input ports creates an optical AND gate, with a twofold advantage over other schemes based on the coupling of polarized gap solitons in Bragg gaps^{5,6}: Our gate is much shorter and requires less energy. The gate works as follows: Forward-traveling light in the bottom (top) channel guide can couple, via the resonators, to backward-traveling light in the top (bottom) guide. In the absence of nonlinearity, the structure highly reflects light with a frequency near the resonance of the microresonators.^{1,2,4} This reflection occurs because light accumulates a phase that is a multiple of 2π in one round trip through the resonator, and hence the coupling of light from one channel guide to the other is resonantly enhanced. In the presence of nonlinearity, light of high intensity will experience nonlinear phase accumulation through self-phase modulation and cross-phase modulation. We consider the situation in which one pulse of high intensity, injected into either the top or the bottom channel, is highly reflected despite its self-phase modulation. However, when pulses are injected into the top and bottom channels simultaneously, the added phase accumulation that results from cross-phase modulation is sufficient to switch off the resonance, so the structure becomes highly transmitting.

First consider one cell of the system [Fig. 1(b)] in the absence of nonlinearity or loss. Light couples between the channel guides and the resonators^{3,4} near the two large filled circles in Fig. 1(b), which we call the coupling points. In terms of coupling coefficients σ and κ , we have⁷

$$\begin{bmatrix} E_3 \\ E_1 \end{bmatrix} = \begin{bmatrix} \sigma & i\kappa \\ i\kappa & \sigma \end{bmatrix} \begin{bmatrix} E_4 \\ E_2 \end{bmatrix}, \quad (1)$$

where fields E_m are shown in Fig. 1(b); an equivalent result obtains at the top coupling point. To conserve energy, the coupling coefficients satisfy $|\sigma|^2 + |\kappa|^2 = 1$ and $\sigma^*\kappa = \sigma\kappa^*$. Away from the coupling points, the only effect of propagation is the accumulation of phase. We assume that propagation constant $\nu = n_{\text{eff}}\omega/c$ is equal for the channel guides and the microresonator; here ω is the frequency of the light and n_{eff} is the effective linear index of refraction of the waveguide. Combining the phase accumulation with the coupling matrices [Eq. (1)], we determine a transfer matrix that

relates the fields at $z = 0$ of the cell to the fields at $z = d$ (Refs. 2 and 3):

$$\begin{bmatrix} l(d) \\ u(d) \end{bmatrix} = \frac{1}{t} \begin{bmatrix} t^2 - r^2 & r \\ -r & 1 \end{bmatrix} \begin{bmatrix} l(0) \\ u(0) \end{bmatrix}, \quad (2)$$

where l and u are indicated in Fig. 1(b) and where we introduce a transmission coefficient, $t(\omega) = \sigma\{\exp[i\phi(\omega)] - 1\} \exp(i\nu d) / \{\sigma^2 \exp[i\phi(\omega)] - 1\}$, and a reflection coefficient, $r(\omega) = (1 - \sigma^2) \exp[i\phi(\omega)/2] \exp(i\nu d) / \{\sigma^2 \exp[i\phi(\omega)] - 1\}$. The quantity $\phi(\omega) = 2\pi\omega/\omega_r$ describes the phase accumulated by light propagating once around the resonator; for a resonator of radius ρ the fundamental resonant frequency is $\omega_r = c/(n_{\text{eff}}\rho)$.

With this transfer matrix we can determine the linear transmission spectrum for the AND gate by using $n_{\text{eff}} = 3$ and geometric parameters $2\pi\rho = 26 \mu\text{m}$ and $d = 16 \mu\text{m}$. In Fig. 2 we plot the transmission for a one-cell (solid curve) and a 5-cell (dashed curve) structure in the vicinity of $\lambda = 1.5294 \mu\text{m}$, which corresponds to the 51st resonance of the resonators. The structures are linearly apodized such that for the first and last cells $\sigma = 0.99$, whereas for the middle cells $\sigma = 0.98$ (the structure with one cell has $\sigma = 0.98$). Without this apodization, the oscillations that are evident at the low-wavelength edge of the 5-cell structure would be far worse. At the low-wavelength edge,

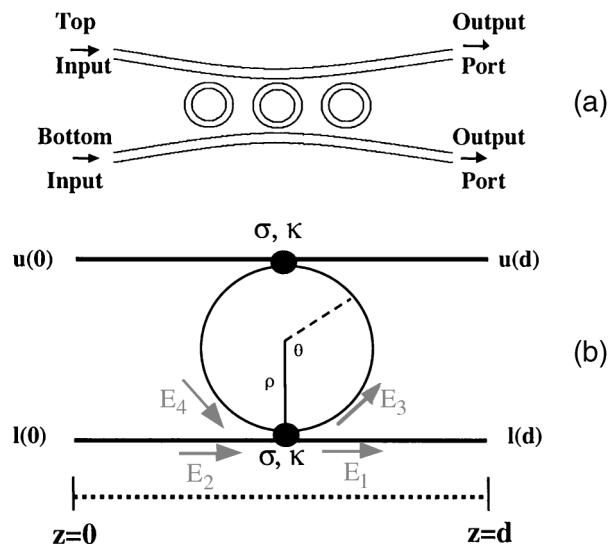


Fig. 1. (a) Schematic of an AND gate with three cells, (b) schematic of one cell of the system.

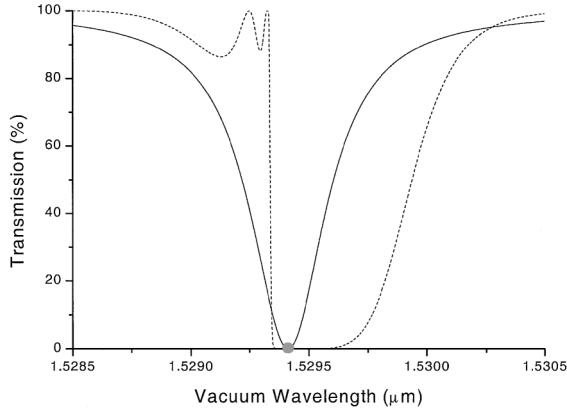


Fig. 2. Continuous-wave transmission spectra for a 1-cell (solid curve) and a 5-cell (dashed curve) structure. The large filled circle indicates the resonant frequency of the microresonators.

used for switching in the presence of positive nonlinearity, the spectrum for the 5-cell structure switches from low to high transmission over a small wavelength range, whereas the 1-cell structure shifts more gradually. Although the 1-cell structure can be used as an AND gate, the contrast between the 0 and 1 states would be quite poor; we concentrate on longer structures in what follows.

We now simulate optical pulse propagation in the presence of both nonlinearity and loss, using a numerical technique described elsewhere.⁴ We consider two pulses injected in the forward direction, one in a top mode and the other in a bottom mode. In a top (bottom) mode, the energy propagates in the forward direction in the top (bottom) channel and in the backward direction in the bottom (top) direction. In the resonators, the energy in the top (bottom) mode circulates in the clockwise (counterclockwise) direction. We define fields $A_T(\zeta, t)$ and $A_B(\zeta, t)$, where ζ is a generalized length variable and where the subscripts T and B indicate a top or a bottom mode, respectively. In the channel waveguides, $\zeta = z$; in the resonator, $\zeta = \rho\theta$. The fields are normalized such that their square modulus gives the intensity in the field. Away from the coupling points, a pulse will propagate with group velocity c/n_{eff} and accumulate linear and nonlinear phase, the latter through self- and cross-phase modulation which are characterized by the nonlinear index-of-refraction coefficient n_2 . We neglect other nonlinear effects, such as third-harmonic generation and four-wave mixing, which are not phase matched and hence should be negligible. Linear loss, two-photon absorption, and three-photon absorption are characterized by coefficients α_1 , α_2 , and α_3 respectively. Thus, away from the coupling points,

$$\begin{aligned} A_j(\zeta, t + \delta t) = & i \frac{\bar{\omega}}{c} (\delta \zeta) (n_{\text{eff}} + n_2 J_j) A_j(\zeta - \delta \zeta, t) \\ & - \frac{1}{2} (\delta \zeta) (\alpha_1 + \alpha_2 J_j + \alpha_3 K_j) \\ & \times A_j(\zeta - \delta \zeta, t), \end{aligned} \quad (3)$$

where

$$J_j = |A_j(\zeta - \delta \zeta, t)|^2 + 2|A_{\bar{j}}(\zeta - \delta \zeta, t)|^2, \quad (4)$$

$$K_j = |A_j(\zeta - \delta \zeta, t)|^4 + 3|A_{\bar{j}}(\zeta - \delta \zeta, t)|^4, \quad (5)$$

with $\bar{j} = T(B)$ when $j = B(T)$; $\bar{\omega}$ is the carrier frequency of the pulse, and we have introduced $\delta \zeta$ and $\delta t = \delta \zeta / (c/n_{\text{eff}})$, the discretization length and time steps, respectively. It is apparent from Eq. (3) that the AND gate is insensitive to the relative phase of the two input pulses. At the coupling points we use matrix equation (1) to shift energy between the channel guides and the resonators. For simplicity we assume that there is no nonlinearity about the coupling points and that no loss is incurred during the coupling.

We consider Gaussian pulses with 100-ps FWHM intensity and a carrier vacuum wavelength $\lambda = 1.5294 \mu\text{m}$ (large filled circle in Fig. 2).⁸ We take $n_2 = 1.1 \times 10^{-4} \text{ cm}^2/\text{GW}$, $\alpha_2 = 0.05 \text{ cm}/\text{GW}$, and $\alpha_3 = 0.08 \text{ cm}^3/\text{GW}^2$, consistent with $\text{Al}_{0.18}\text{Ga}_{0.82}\text{As}$, a material used in nonlinear waveguiding applications.⁸ We use a linear loss of 1 dB/cm ($\alpha_1 = 0.23 \text{ cm}^{-1}$), consistent with the observed loss in straight waveguides fabricated with AlGaAs.⁹ Losses to date in resonator structures have typically been much higher than this, owing to fabrication problems rather than to the fundamental limit imposed by bending loss,¹⁰ which is much less than 1 dB/cm.

We simulate 5- and 10-cell structures, apodized as discussed above, and introduce a contrast ratio $\gamma(I_p)$, where I_p is the peak intensity of the input pulse. This is the ratio between the energy transmitted (per pulse) by the device for a Gaussian pulse of peak intensity I_p in the presence of a sister pulse of the same form in the neighboring channel, to the corresponding transmission of the same pulse in the absence of a sister pulse. In Fig. 3(a) we plot $\gamma(I_p)$ for the 5-cell (solid curve) and 10-cell (dashed curve) structures; the maximum value of γ , γ_{max} , is slightly larger for the 10-cell structure than for the 5-cell structure and occurs at $I_p \approx 11 \text{ MW}/\text{cm}^2$ for both structures. The value of I_p that corresponds

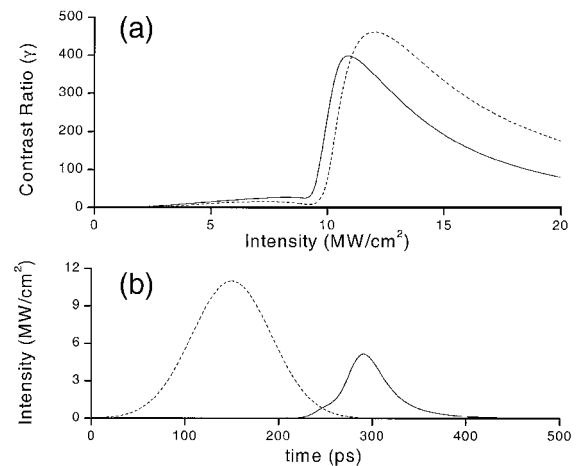


Fig. 3. (a) AND gate contrast ratio, $\gamma(I_p)$, for a 5- (solid) and a 10- (dashed curve) cell structure. (b) Input (dashed curve) and output (solid curve) pulses along the bottom channel of the five-cell AND gate at $I_p = 11 \text{ MW}/\text{cm}^2$, which corresponds to the maximum value of $\gamma(I_p)$.

to γ_{\max} is slightly lower than the switching threshold for the 1-pulse situation but well beyond the switching threshold for the 2-pulse situation. For larger values of I_p the 1-pulse situation passes threshold and starts transmitting, so the contrast ratio decreases. Although we have used two identical Gaussian pulses as input, a stronger pulse could be used to control the transmission of a weaker pulse. The two structures have a roughly equal γ_{\max} because the sharper transmission spectrum of the longer structure is balanced by a larger total loss; the peak transmission of the 5- (10-) cell structure at γ_{\max} is 27% (14.5%). In Fig. 3(b) we plot the input (dashed curve) and output (solid curve) pulses along the bottom channel waveguide at γ_{\max} for the 5-cell structure. The output pulse is compressed to 48 ps and has experienced a group delay of 140 ps. For our 80- μm device this result indicates an effective group velocity of 0.57 $\mu\text{m}/\text{ps}$, which is only 0.57% of the expected group velocity in a medium with $n_{\text{eff}} = 3$. The large group delay occurs because the light is trapped in the resonators for a long time; the consequent enhancement of the local intensity⁷ partly explains the low switching threshold required for the device.

To underscore the effectiveness of this AND gate operation we used the nonlinear coupled-mode equations to simulate an AND gate operating in an isotropic Bragg grating, using the two polarizations as the inputs to the device. Such structures have been observed in optical fibers,⁶ but to maximize the effect of nonlinearities one would likely use a chalcogenide fiber that would have an n_2 comparable to that of AlGaAs. To make a comparison that emphasizes the difference in the device structures rather than in material parameters, we assume the same n_2 and loss coefficients in our devices and choose a grating length of 2 cm with $\Delta n/n = 8 \times 10^{-4}$ to give the same stopgap with as our microresonator structures. Using input pulses of exactly the same temporal width, we found that the threshold for AND gate operation was 150 MW/cm², which is 15 times larger than in the microresonator structures. Furthermore, as the cross-sectional area of a microresonator structure is $\sim 0.3 \mu\text{m}^2$, whereas that of a single-mode fiber grating is $\sim 50 \mu\text{m}^2$, the energy requirements

for the microresonator structure are ~ 2500 times lower.

In conclusion, we have numerically demonstrated the feasibility of using two waveguides coupled by microresonators as a logical AND gate. Our simulations included realistic loss and nonlinear parameters and indicated that the AND gate effect should be observable in short (approximately 100–200- μm) structures with $\sim 10\text{-MW}/\text{cm}^2$ peak input intensity in each arm of the gate. We have verified that the device operation is significantly enhanced relative to an equivalent Bragg system. Finally, we note that although both our device and the Bragg system would work with much shorter pulses, they would then require a much wider gap, and the threshold required for switching would be substantially increased.

This research was supported by the Natural Sciences and Engineering Research Council of Canada and by Photonics Research Ontario. S. Pereira's e-mail address is pereira@physics.utoronto.ca.

References

1. B. E. Little, S. T. Chu, J. V. Hryniewicz, and P. P. Absil, *Opt. Lett.* **25**, 344 (2000).
2. A. Melloni, *Opt. Lett.* **26**, 917 (2001).
3. S. Pereira, J. E. Sipe, J. E. Heebner, and R. W. Boyd, *Opt. Lett.* **27**, 536 (2002).
4. S. Pereira, P. Chak, and J. E. Sipe, *J. Opt. Soc. Am. B* **19**, 2191 (2002).
5. S. Lee and S.-T. Ho, *Opt. Lett.* **18**, 962 (1993).
6. D. Taverner, N. G. R. Broderick, D. J. Richardson, M. Ibsen, and R. I. Laming, *Opt. Lett.* **23**, 259 (1998).
7. J. E. Heebner, R. W. Boyd, and Q.-H. Park, *J. Opt. Soc. Am. B* **19**, 722 (2002).
8. Optical bistability comes into play only when the carrier frequency of the pulse is positively detuned from the resonance frequency of the resonator. See P. Chak, J. E. Sipe, and S. Pereira, *Opt. Commun.* **213**, 163 (2002).
9. A. Villeneuve, C. C. Yang, P. G. J. Wigley, G. I. Stegeman, J. S. Aitchison, and C. N. Ironside, *Appl. Phys. Lett.* **61**, 147 (1992).
10. V. Van, P. P. Absil, J. V. Hryniewicz, and P.-T. Ho, *Opt. Lett.* **19**, 1734 (2001).